

Planar laser-induced fluorescence measurement of the angular pattern of the cone-shaped spray

Oleg Gobyzov*, Mikhail Ryabov, Konstantin Inzhevatkin, Artur Bilsky, Dmitriy Markovich

¹Kutateladze Institute of Thermophysics, Siberian Branch of Russian Academy of Sciences, 630090, Novosibirsk, Russia

Abstract. In the present work, a PLIF-based approach for a large cone-shaped spray patterning is presented and experimental results of its application are discussed. The patterning approach is based on simple time-averaged PLIF imaging. Special attention is paid to the image and data processing in order to simplify a patterning results interpretation. Experimental testing was performed on a water spray, formed by centrifugal nozzle at atmospheric ambient pressure. Circumferential relative concentration profiles in spray crosswise plane are presented in the paper and their validity is analysed.

1 Introduction

Spray testing is one of the important problems for many different practical applications. Despite the many years of development and a large number of different techniques developed for the task, spray testing still remains challenging. One of the major tasks in spray testing is a spray patterning, in other words – acquisition of spatial structure of a spray. In industrial measurements, patterning is usually performed with mechanical patternators that collect portions of the spray into special collector bins. Mechanical patternators measure time-averaged mass-flow rate within the section of the spray.

This technique is straightforward and robust, but have certain inherent disadvantages. For example, mechanical patternators lack flexibility and often a specific configuration of collectors is required for different nozzles. Besides that, their spatial resolution is restricted by the construction and size of the spray collector bins, which often hinders the interpretation of test results. Considering this, an optical patterning is seen as a promising alternative. Optical setups are nonintrusive, more flexible, and can provide data with higher spatial resolution.

A large number of optical methods are available for spray testing: elastic (Mie) scattering, planar laser-induced fluorescence (PLIF), phase-doppler particle analysis (PDPA), time-shift technique, various methods based on laser light extinction or attenuation, and many others. Pointwise techniques, very powerful for in-depth investigation of atomization, in general are not as well suited for the patterning tasks as planar or volumetric techniques. An optical patterning based on the line-of-sight laser light extinction/transmission [1] is one of the specialized optical methods for spray patterning that gained certain recognition. This method employs

tomographic reconstruction and yields local liquid surface area distribution in spray crosssection.

An elastic (Mie) scattering and PLIF has become wide-spread techniques for spray studies as they allow for detailed spatially-distributed measurements and employ rather multipurpose equipment, such as lasers and digital cameras. Additionally, in PLIF the data acquired is directly associated with the volumetric concentration of liquid in the measurement plane.

A large number of examples of spray diagnostics with PLIF and elastic scattering, as well as modifications of these techniques, is presented in papers, yet only a small number of them is focused on the patterning task, i.e. measurements in crosswise plain with quantification of spray structure. For example in [2] a PLIF and Mie scattering patterning of a fuel injector in gas-turbine combustor was performed. Authors employed several optical methods to describe the spray structure and had investigated an evolution of the spray with increase of a distance from a nozzle exit. A circumferential (angular) patterning of a spray generated by an aero-engine atomizer at elevated pressure was presented in [3], though this work did not provide details about experimental technique and data processing. Another example is the work [4], in which authors used dual light-sheet lighting to reduce the laser light attenuation effect and validated the optical patterning results with mechanical patternator measurements.

In the present work, a PLIF-based approach for a large cone-shaped spray patterning is presented and experimental results of its application are discussed. Sprays of such kind are quite common in fire extinguishing systems, irrigation systems and in some of the continuous fuel injection nozzles.

* Corresponding author: oleg.a.g.post@gmail.com

2 Experimental setup and measurement system

PLIF system used in experiments included a continuous DPSS laser (532 nm emission wavelength) with light-sheet forming optics and a CCD-camera with a lens and a colored glass filter used to suppress light at emission wavelength. A spray was formed by a centrifugal nozzle, a diameter of the spray in the patternation plane was about 350 mm. A nozzle was connected to a supply line through a straight swivel fitting which allowed to revolve a nozzle around its axis of symmetry. A distilled water doped with a small amount of Rhodamine 6G luminophore (30 μg per liter) was used as a working liquid.

Patternation by means of PLIF assumes that spray is illuminated with a light sheet aligned in a horizontal plane, orthogonal to the spray nozzle axis. Usually, a collimated light sheet is used to avoid the energy variation along the light-sheet, but forming a collimated light-sheet requires optical elements of a size, comparable to the size of the measurement area and thus technically challenging in case of large spray. For this reason, a divergent light sheet was employed.

A camera was placed above the spray nozzle at an angle to the measurement area. In this case, as the size of the spray is comparable to the distance from the measurement plane to the lens, different light collection angles for different parts of the spray, as well as the different light path length through the spray volume can affect a PLIF image. On the whole, the selected PLIF system configuration was simple in realization but had many potential sources of error that had to be corrected through the imaging and data processing procedures. A scheme of the PLIF experiment is shown in figure 1.

During measurements, a nozzle was rotated around its axis of symmetry with a step of 15° , and for each position (24 positions in total) a 16-bit image with a long exposure of about 1 second was captured. To perform a perspective distortion correction (geometric reconstruction) an image of a calibration target placed in a light-sheet plane was captured before measurements. Set of images captured at different nozzle rotation angles θ were used in correction procedures and for estimation of the measurement's uncertainty.

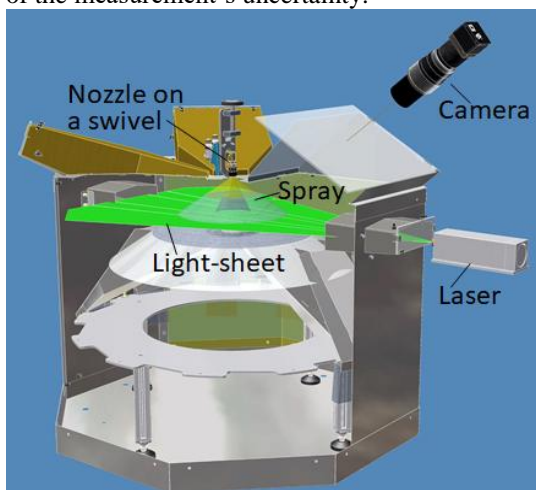


Fig. 1. Scheme of the experiment and optical setup.

3 Data processing

The data processing consisted of several steps: image geometric reconstruction, identification of the spray pattern center, coordinate system transformation and integration of the signal, correction and normalization of the spray angular profile.

Geometric reconstruction was performed using a calibration target image and a back-projection algorithm with a second-order polynomial model [5].

The geometric reconstruction procedure was followed by a spray pattern center search. There can be various definitions of the spray center and, therefore, different methods for estimation of its position. The spray center can be fixed beforehand, as in circumferential mechanical patternators, assuming that the nozzle and measurement area are perfectly aligned and the spray is not tilted. In other cases, a center can be set manually by the operator. Sometimes a centroid is considered as a spray center, as in [3], but in a spray with strong local nonuniformities, centroid position will be biased from the 'geometric' center of the spray pattern. Assuming that an 'expected' spray shape is known in advance and that its variations are relatively small a shape approximation can be employed. For example, for hollow or filled cone sprays an approximation by a circle or ellipse can be feasible. In the present work, a right circular hollow cone spray was an 'expected' shape in experiments and a circle approximation in the measurement plane was employed. To perform an approximation, two image brightness maxima positions (one maximum in each half of the image) over each of the image rows and columns were detected, and then positions of the maxima were approximated by a circle. Obviously, outliers can appear in the list of image brightness maxima due to the spray shape deformation, stray light in the image or hot pixels in the sensor. Strong outliers bias the simple least-squares fitting, thus a more robust RANSAC [6] circle parameters estimation was used to prevent bias. To define an outer boundary of the spray pattern, a circle radius was increased until the average intensity over its perimeter was smaller than a threshold value (which was set slightly above the background brightness).

After the center and a bounding radius of a spray were evaluated, a transformation of the image to the polar coordinates with a coordinate system center at a found circle center, and numerical integration of the image intensity over the sectors with defined central angle was performed.

Preliminary tests of the processing procedure on synthetic images was performed to ensure its viability. Synthetic images were ring-shaped patterns with radial intensity gradient, with introduced Gaussian local shape and brightness distortions, random brightness noise up to 5% of the maximum brightness, and nonuniform stray light distribution with brightness from 0 up to 10% of the maximum signal level. An example of the synthetic image and corresponding circumferential profile are shown in fig 2.

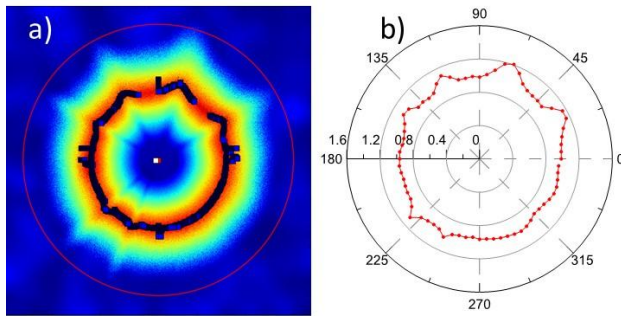


Fig. 2. Example of synthetic image (a) with identified valid maxima, center and outer boundary, and corresponding circumferential profile (b).

The processing procedure proved to be robust towards introduced distortions and yielded the center position with the precision better than 2 pix (0,2 % of the synthetic image size and about 0,4 % of the characteristic ring diameter). From the working principle of the RANSAC algorithm, it is expected to remain stable until large-scale structured spray shape distortions take place, or, in other words, until a concurrent fitting model appears.

4 Experimental results and discussion

The described processing procedure was applied to the set of experimental images. To suppress brightness variations produced by an excitation light intensity variations (figure 3) a light-sheet correction procedure was employed beforehand. To perform the correction, a test section was filled with a fine mist of water doped with luminophore using a Laskin nozzle aerosol generator. After the mist got settled in a test section, a set of PLIF images of the mist were captured and a standard light-sheet correction of spray images was performed as follows:

$$I_c(x, y) = I_0(x, y) \frac{\bar{I}_s}{I_s} \quad (1)$$

where I_0 is the initial image brightness, I_s is the light-sheet brightness at the same pixel and \bar{I}_s is the light-sheet brightness averaged over the measurement area. After a light-sheet correction an image is assumed to represent a distribution of relative concentration of the liquid.

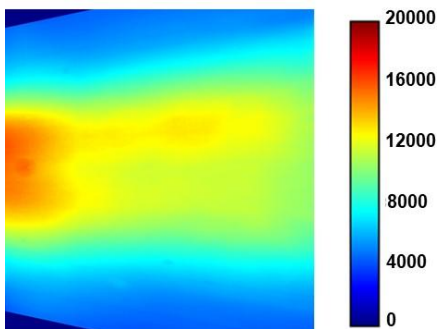


Fig. 3. Light-sheet brightness distribution.

An example of the raw PLIF image of the spray crosssection and the result of the geometric reconstruction and light-sheet correction are shown in figure 4. From the image, it can be seen that a spray pattern shape is

close to circular in general with a large number of local intensity variations.

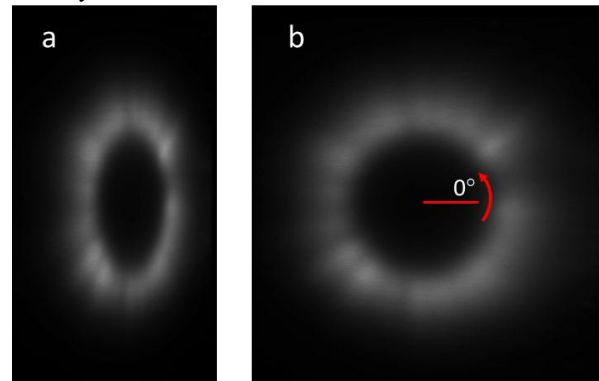


Fig. 4. a) A raw PLIF image for nozzle rotation angle $\theta=0^\circ$, b) PLIF image after geometric reconstruction and light-sheet correction.

The center and radius search procedures applied to the images yielded qualitatively good results, yet there was no proper technique to quantify a precision of center identification in the experimental image.

Besides the signal variations seen in the images, the acquired circumferential spray pattern also contained strong large-scale distortions, which remained stationary with the rotation of the nozzle on a swivel (see fig. 5). They were identified as the artifacts of the optical arrangement: as it was noted in ‘experimental setup’ section, there is a number of effects that can lead to such distortions. These distortions, which remained after the light-sheet correction, were most likely related to the variation of the light path length through the spray volume for different parts of the measurement area and light-sheet attenuation in the bulk of the spray.

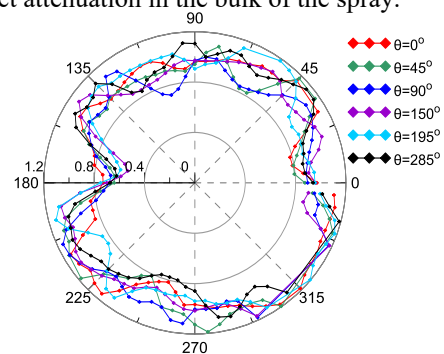


Fig. 5. Spray angular profiles with spurious distortions for different nozzle rotation angles.

Assuming that flow conditions inside the feed line do not change with nozzle rotation, spray pattern features will rotate accordingly while spurious brightness variations should remain stationary. This allows to use the circumferential profile, averaged over the different nozzle rotation angles, as a reference to normalize profiles for separate rotation angles in order to eliminate the rest of the spurious brightness variations as follows:

$$Q(\varphi, \theta_k) = \frac{q(\varphi, \theta_k)}{N_\theta} \sum_i q(\varphi, \theta_i) \quad (2)$$

where Q is the normalized relative concentration within the sector φ , q is not normalized relative concentration, θ is the nozzle rotation angle and N_θ is the total number of rotation angles.

To test this approach profiles averaged over 24, 12, 6 and 3 rotation angles θ were calculated (see fig. 6). Profiles averaged over 24 and 12 rotation angles match each other quite well, which indicates a sufficient number of samples in the statistic. These profiles feature only large-scale variations. Profiles averaged over a smaller number of rotation angles show local variations and worse match to each other and to the profiles with larger statistics. Apparently, a sufficient number of samples (nozzle rotation angles) may vary depending on the optical setup and a spray structure.

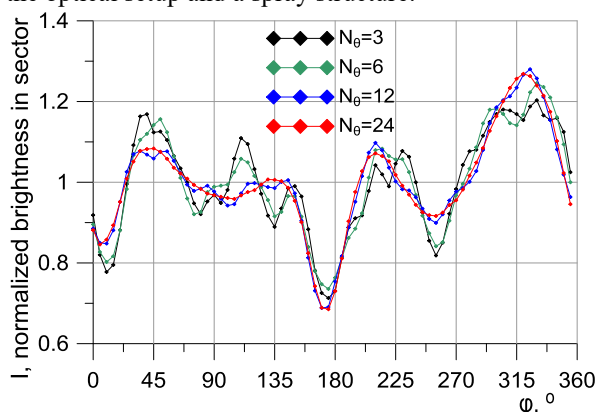


Fig. 6. Angular profiles averaged over different number of samples.

In figure 7b a normalized angular relative concentration profiles for 0° and 90° nozzle rotation angles are shown. Profiles match closely and demonstrate common features of the spray pattern, which can be also noticed in raw images (see fig 3). Therefore, it can be concluded that the proposed correction procedures allowed to eliminate most of the error sources and yield circumferential profiles that clearly reveal the angular nonuniformity of the spray.

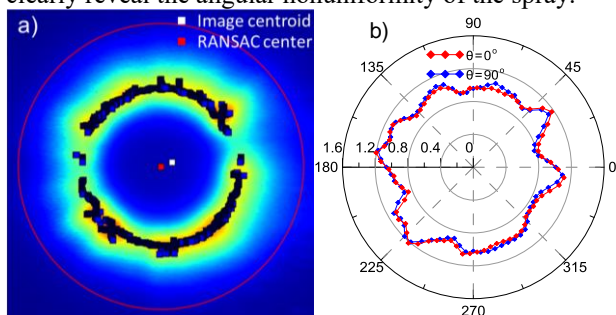


Fig. 7. PLIF-image (a) with identified center and radius and angular relative concentration profiles for 0° and 90° nozzle rotation angles (b). A 90° profile is revolved to match the orientation of 0° -profile for better comprehension.

To quantify a measurement error an RMS of the relative concentration was evaluated from profiles for 24 separate nozzle rotation angles. An RMS of the relative concentration was less than 10% for the profile with sectors division $\Delta\varphi=5^\circ$ (see figure 8). Note that error could partially come from the flow conditions changes and error in setting the nozzle rotation angle, so this value should be considered as an upper boundary of the measurement error.

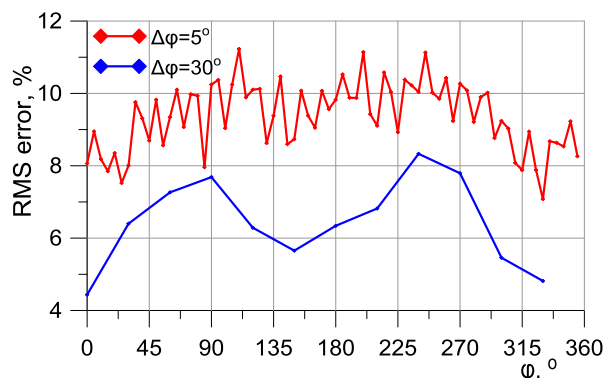


Fig. 8. RMS Error of angular relative concentration distribution for sectors division $\Delta\varphi=5^\circ$ and $\Delta\varphi=30^\circ$.

5 Conclusion

A method for PLIF circumferential patterning of the large cone-shaped spray was developed. The method benefits from low equipment requirements and relatively free camera positioning. In current realization it is not meant for application as a sole patterning instrument, as some of the error sources are yet to be considered. Nevertheless, it can be used as a supplementary method for more informative spray testing.

In the future work, the method can be substantially improved by introducing such techniques as a correction of planar laser-induced fluorescence distributions for local nonuniform laser attenuation and suppression of secondary reflections.

The main disadvantage of the procedure is the need for a large number of PLIF-images captured at different nozzle rotation angles. This part can be also improved, for example by rotating the measurement system on a rotational stage instead of rotating the nozzle.

Acknowledgements: The research was supported by the Russian Science Foundation (Grant No 19-79-30075).

References

1. J. Lim, Y. Sivathanu, V. Narayanan, S. Chang, *Atomization and Sprays*, **13**, 27 (2003)
2. R. J. Locke, Y. R. Hicks, R. C. Anderson, M. M. Zaller, *Combustion Science and Technology*, **138**, 297 (1998)
3. M.K. Lai, W.G. Freeman, P.R. Yankowich, J.D. Bryant, P. Walterscheid, *Proceedings of the ASME Turbo Expo 2004*, **665** (2004).
4. K. Jung, H. Koh, Y. Yoon, *Meas. Sci. Technol.* **14**, 1387 (2003)
5. S.M. Soloff, R.J. Adrain, Z-C. Liu, *Meas. Sci. Technol.*, **8**, 1441 (1997)
6. M. Fischler, R. Bolles, *Communications of the ACM*, **24**, 381 (1981)